

Impact of Coal Mine Waste Aggregates (CMWGs) as a Mixing Component on Mechanical Properties of Concrete

O. Aboutaybi* and B. Yang

L2mgc-CY Paris university, Neuville sur oise, France

Email: oumayma.aboutaybi@cyu.fr (O.A); boyuan.yang@cyu.fr (B.Y)

*Corresponding author

Abstract—Over 50 million tons of solid waste, primarily from hard coal mines are generated in Poland annually. This type of waste, called Coal Mine Wastes (CMWs), can be found across the country due to mining activities. CMWs triggers several environmental problems such as groundwater contamination, primarily characterized by heightened chloride salinity, acid generation, and sulfur content. The main objective of this study is to examine the possibility to substitute natural aggregates in concrete with CMWs. Characterization of coal-mining waste physico-chemical properties and assessment of short-term and long-term structural concrete behaviors such as compressive strength, splitting tensile strength, bulk density, water absorption, and porosity were considered. Mechanical results show an obvious decline of concrete fabricated with CMWGs, a substitution of 10% natural sand and 30% natural coarse aggregate proves sufficient to elaborate C40/50 concrete. Moreover, the incorporation of coal waste negatively impacts the density and the porosity of concrete.

Keywords—coal mine waste aggregates, concrete, mechanical properties, recycling, circular economic, untreated waste coal aggregates

I. INTRODUCTION

Over the past few decades, the construction industry has grappled with various challenges, including the depletion of natural resources, heightening energy consumption, and the generation of excessive waste materials, all of which directly impact the environmental balance. Recycling has emerged as a promising solution to address environmental concerns within the field of civil engineering, particularly in European countries like Poland, where the challenge currently is managing 812 million tons of waste from coal mines waste (CMWs), as reported by the Central Statistical Office (GUS 2019). Several studies have explored the feasibility of incorporating CMWs into concrete or mortar as partial substitution of cement, or sand and gravel, aiming to enhance its mechanical properties [1–8]. Yu *et al.* [9] have also verified that incorporating coal mine waste aggregates (CGC) alters the setting time and hydration

mechanism of concrete, mechanical properties are likewise impacted. Specifically, they observed a decrease in the flexural, compressive, and splitting strengths of mortar beyond a substitution rate of 25% with CGC. Wu *et al.* [10] prepared several concrete series with varying replacement levels (25%, 50%, 75%, and 100%) of sand and gravel. They observed a decrease in compressive strength and concrete density as substituting natural aggregates with coal mine waste aggregates increased. However, an increase was detected in water permeability, which could be explain by higher porosity, especially connected pores and water absorption of coal mine waste aggregates. In the study conducted by Karimaei *et al.* [11], the impact of untreated coal mine waste as a partial replacement for natural coarse aggregates (NCA) and natural fine aggregates (NFA) on concrete properties have been assessed. The results revealed that substituting 25% of natural fine aggregates (NFA) with untreated coal mine waste aggregates (RCGA) led to a 29% decrease in compressive strength and 20% in modulus elasticity. It's commonly accepted that the use of coal mine wastes as a substitute for natural fine aggregates has a detrimental effect on the mechanical properties of concrete. It is imperative to further research in order to gain a better understanding of the implications of incorporating coal mine waste in concrete. Exploring solutions to improve the mechanical properties of CMWs concrete and its durability is essential. This could involve investigations about the optimal proportions of coal mine waste, the utilization of specialized additives to solidify concrete performance, and understanding the behavior of concrete in the face of an aggressive environment. By advancing such research endeavors, we can pioneer more sustainable practices in construction industry, thereby mitigating the environmental footprint associated with coal mine waste.

This research is being carried out as part of the RFCS-2019 MINRESCUE Project, focusing the impact of incorporating Coal Mine Waste (CMW) aggregates on the mechanical properties of concrete. The reference concrete designed for precast applications has a strength class of C40/50 and a consistency class of S4 (20mm-25mm). The substitution approach involves replacing 10% of the volume of natural sand and 30% of natural

Manuscript received June 31, 2024; revised July 19, 2024; accepted accepted September 11, 2024; published November 26, 2024.

gravels with CMW aggregates. This article presents a comparative study between reference concrete (C-REF) and concrete incorporating coal mine waste.

The goal of this study is to assess the feasibility of integrating untreated waste materials from coal mines, particularly sand and gravel, into the formulation of concrete mixtures tailored for constructing curved structural elements. The main objective is to identify the optimal utilization of additives derived from coal mine waste, comprising sand and gravel, and to evaluate their impact on the strength properties of the concrete used in mine construction over time.

II. MATERIALS AND METHODS

A. Materials

The CMWs gravel (MINRE-WALB-004 5/18 mm) and sand (MINRE-WALB-004 0/4 mm) used to prepare concrete specimens are supplied by the Poltegor Institute in Poland, Natural sand (SN 0/4), Natural gravel (GN 5/18), Cement (CEM II/A-LL 42.5R; with density 3.05 Kg/m³), limestone fillers (2.72 Kg/m³), and superplasticizer (0.4 Kg/m³). Several tests were conducted according to the NF P 18-545 standard to verify the compliance of CMW. Table I presents the various physical properties of the materials used, and the particle size distribution of the aggregate is illustrated in Fig. 1. In terms of chemical composition (Table II), the coal waste was primarily composed of SiO₂, Al₂O₃, and Fe₂O₃, accounting for weight percentages of 34.03%, 17.62%, and 5.75%, respectively.

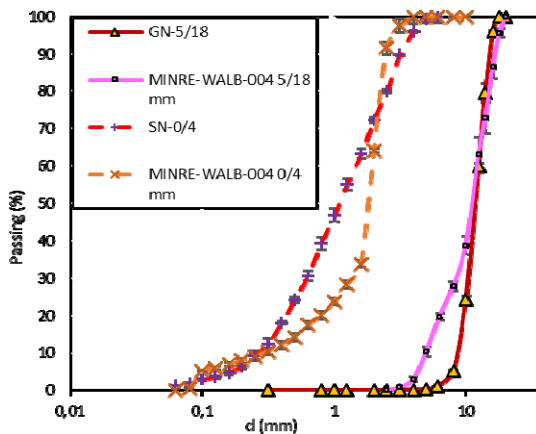


Fig. 1. Particle size distribution.

TABLE I. PHYSICAL PROPERTIES OF THE AGGREGATES

Property	Standard	SN 0/4	MINRE -WALB- 004 0/4mm	GN- 5/18	MINRE- WALB- 004 5/18mm
Bulk density (kg/m ³)	NF EN 1097-6	2.68	2.17	2.7	2.16
W _{A24h}	NF EN 1097-6	1.4	2.6	1.1	7.2
F _M	NF EN 933-3	3.5	3.8	-	-
C _U	NF EN 933-3	6.4	6.3	1.6	1.5
C _C	NF EN 933-3	1	2.4	1	1

TABLE II. CHEMICAL STRUCTURE OF COAL MINE WASTE

Element	Quantity (%)
SiO ₂	34.03
LOI	33.7
Al ₂ O ₃	17.62
Fe ₂ O ₃	5.75
K ₂ O	3.52
SO ₃	1.76
MgO	1.25
TiO ₂	1.10
CaO	1.04

B. Methods

Two formulations of conventional concrete are considered for experimental tests: reference concrete (C-REF) with natural aggregate and CMWG concrete (C-F10%-G30%) fabricated by 10% of MINRE-WALB-004 0/4 mm sand and 30% of MINRE-WALB-004 5/18 mm gravels volume substitution, the water/cement ratio was maintained constant for all formulation, 0.45 shown in Table III.

TABLE III. FORMULATION OF CONCRETE

Material	C-REF	C-F10%-G30%
	Quantity Kg/m ³	
SN 0/4	938	844
GN-5/18	879	615
MINRE-WALB-004 0/4 mm	-	78
MINRE-WALB-004 5/18 mm	-	200
Filler DOP N1040	59	59
CEMENT II 42.5	326	326
Water	158	158
Superplasticizer DYNAMON NRG1030	2	2

Cylinder specimens (11mm×22mm) were tested at the ages of 7, 14 and 28 days according to the standards NFEN 12390-3 and 12390-6.

The compression tests were carried out using a SCHENCK hydraulic servo-controlled press with a capacity of 3500 KN, and they were conducted at a loading rate of 0.5 MPa/s (NF-EN 12390-3). Before testing, the specimens underwent a meticulous surfacing process using a surfacing mortar certified to ISO-9001 standards. This mortar was heated to 180 °C for liquefaction in an oil bath from the MAGMAX-3R brand. Hot sulfur was poured onto the surfacing square, and the specimen was positioned vertically. Conversely, the tensile strength tests were carried out at a loading rate of 0.05 MPa/s (NF-EN 12390-6).

The Water absorption measurement was applied on 10cm×10cm×10cm cube at the age of 28 days following the NF P18-459 standard. The samples were subjected to a vacuum for 4 h at a pressure of 25 mbar, followed by immersion in water at the same pressure for 44 h. After

48 h, the mass was determined through hydrostatic weighing. Subsequently, the dry mass was determined after drying at a temperature of 60°C until a constant mass was achieved (with a difference of 0.05% between two consecutive weighing conducted 24 h apart). The Water absorption measurement was calculated using the following Eq. (1):

$$WA_{48h}(\%) = 100 \times (M_{air} - M_{dry}) / M_{dry} \quad (1)$$

M_{Air} is the mass in air of the saturated sample in kg;

M_{dry} is the mass of the sample dried at 60°C in kg;

1) Fresh concrete properties

Slump test as shown in Fig. 2 (a) and (b) for C-REF and C-F10%-G30% was conducted. The slump value for reference concrete (C-REF) is 23.2 mm and 19mm for C-F10%-G30%. The fluidity of C-F10%-G30% decreased by 18.1% because of the higher porosity (7.2%) and the irregularities on CMW surfaces. When these particles are incorporated into cement pastes, the porosity allows for increased surface area for interaction with the cement matrix. Moreover, the rough texture of CMW create more contact points and interlocking features between them and the cement matrix. This enlarged surface area facilitates a stronger bond with the cement paste and increase water absorption during the mixing process.



Fig. 2. Slump of specimens at different percentages of replacing aggregate by untreated CMW

In Fig. 3, exothermic evolution during the hydration is presented for both types of concrete, revealing distinctive patterns across five periods. The Initial period (1) is marked by an obvious acceleration of heat release during the dissolution of various ions such as SO_4^{2-} and Al^{3+} , as well as, the initial hydration of C3S, C3A and C4AF forms small initial C-S-H and Aft around the surface of cement grains, limiting further reaction. After this period, the heat hydration rate slows down due to the higher concentration of Ca^{2+} , OH^- ions. Meanwhile, the protective layers of outer C-S-H and C-S-H needles continue to develop on cement grain surfaces and create an aqueous transition zone due to their contact with the anhydrous core. Once Ca^{2+} and OH^- ions reach the critical level, the C-S-H film is turned into C-S-H gel with higher porosity and Ca content[12]. This transformation facilitates a relatively unlimited diffusion of calcium, silicate, and hydroxide ions, creating a concentration gradient from the protective layer to the transition zone. The induction period (2) finishes when the C-S-H gel is eventually destroyed. The Acceleration period (3)

exhibits an increase in heat release, rapid formation of C-S-H and precipitation of CH, also, gradual dissolution of gypsum and C3A form more ettringite. Portlandite crystallizes into fine platelets, and non-blocking ettringite forms fine needles, contributing to the development of a rigid skeleton. The reduction in the heat evolution observed in C-F10%-G30% is primarily attributed to the dilution effect resulting from a decrease in the C3S content in the cement, limiting its ability to incorporate higher levels of CMW. Additionally, the gradual reaction between aluminosilicates in CMW and calcium hydroxide CH may contribute to the observed trend. The dosage of CMW proves influential, impacting the effective water-to-cement ratio and displaying a nucleation effect due to its low activity. CMW has the potential to reduce the hydration rate of the binder by absorbing significant amounts of Ca^{2+} and water on its spherical particles and also its rerated pozzolanic reaction. Following this, A gradual slowdown in the hydration reaction occurs during the Deceleration phase (4). This stage is dominated by the diffusion of Si^{4+} , Ca^{2+} ions and the transformation of ettringite to monosulfoaluminate [13, 14]. The final Stability period (5) indicates the stabilization of the heat hydration release and the ambient temperature. However, the hydration process will persist slowly for extended period of time [15].

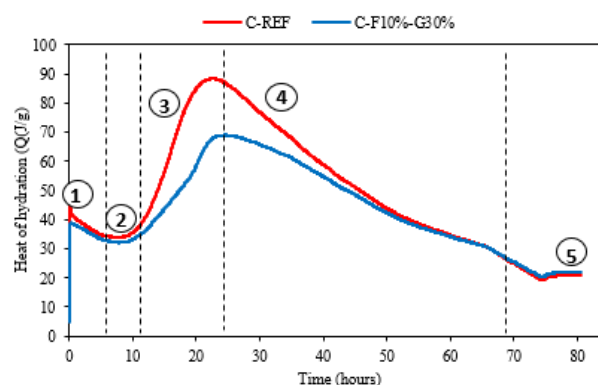


Fig. 3. Evolution of the hydration heat of the different concrete.

2) Concrete dry density and porosity

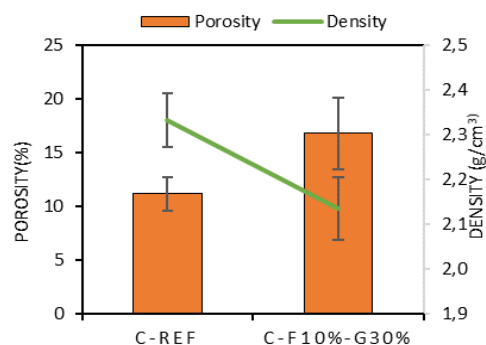


Fig. 4. Bulk density of concrete as function of CMWs ratio.

The porosity and bulk density of concrete were measured after 28 days of curing in water according to standard NF P 18-459, shown in Fig. 4. Results indicate

that the integration of CMWs decreases the density around 9% and increases the porosity of concrete about 33%. This result may due to higher absorption capacity of CMWs (7.2%) and lower density of these waste aggregates. Besides, the angular shape CMW aggregates which leads to obtain concrete containing a higher proportion of CMW.

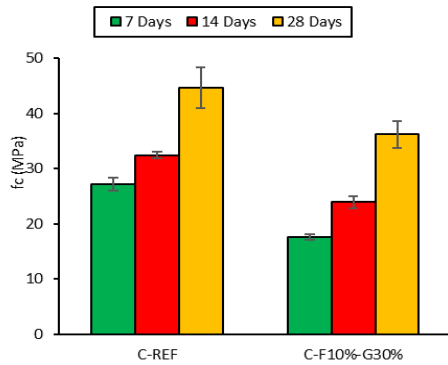


Fig. 5. Compressive strength of concrete at different curing age.

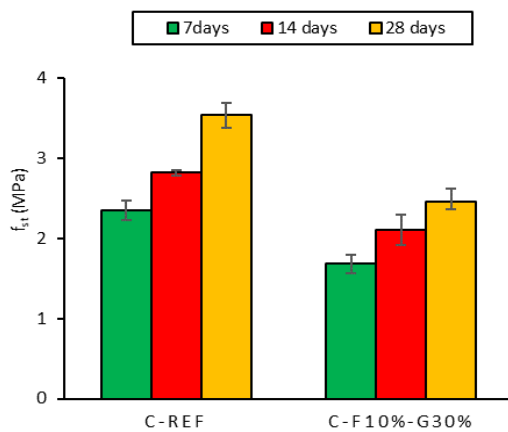


Fig. 6. Splitting tensile strength of concrete at different curing age.

In Fig. 6 and Fig. 7, the evolution of compressive strength and splitting tensile strength of C-REF and C-F10%-G30% was illustrated as a function of curing age. In comparison to the reference concrete, a loss of compressive strength of approximately 36%, 26%, and 19% for the C-F10%-G30% mixes were observed at 7, 14, and 28 days respectively. This decrease may due to, firstly, the brittleness of aggregates as evidenced by a Los Angeles (LA) index of 45% and a micro-Deval (MDE) coefficient of 92% (shown in Table IV), secondly, the significant water absorption capacity of wastes as shown in Table I. The results also revealed a surprise increasing of strength from 3 days to 28 days % for the C-F10%-G30% mix, which turns out about 51.3%, higher than 39% for the C-REF mixes. This strength improvement may due to the activation of pozzolanic components, induced by abundant Si₂O and Al₂O₃ compounds in coal mine waste, result in promoting concrete hydration. A similar improvement was observed for the dynamic elastic modulus of concrete at 28 days, measured with the E-MK2 machine, with a value of 33 GPa for the C-F10%-G30% mix and 46 GPa for the C-REF mixes. Same trend

was observed for the splitting tensile strength (f_{st}): evolution of the tensile strength of concrete over the curing period decrease of the strength with the incorporation of CMW aggregates into the concrete. Compared to the C-REF, the C-F10%-G30% mixes lost approximately 29%, 34%, and 30% after 7, 14 and 28 days. Conversely, tensile strength improves as the hydration reaction of the matrix progresses with the curing age. The findings indicate an improvement in tensile strength from 3 days to 28 days by 20% and 32%.

TABLE IV. THE MDE AND LA COEFFICIENTS FOR THE CMW AND NATURAL AGGREGATES FOR [10-14] GRANULAR FRACTION

Material	Obtained results		NF P 18-545 and NF EN 12620+A1 recommendations	
	LA (%)	MDE (%)	LA (%)	MDE (%)
Natural gravel	19	9	30	25
CMWGs	45	92	40	25

The EC2 model [16] predicts the progression of compressive strength over time. The compressive strength can be estimated for a given age t (named $P(t)$) using Eq. (2):

$$P(t) = P(28) \times \exp(s[1 - (28/t)^{0.5}]) \quad (2)$$

The coefficient “s” varies based on the type of cement (for CEMII, $s=0.2$). According the Fig. 7 and Fig. 8, The prediction of C-REF and F10%-G-30% strengths exhibit disparities compared to the experimental results. The EC2 equations to much overestimated the f_c and f_{st} both for C-F10%-G30%, which may due to the change in the pozzolanic reaction of cement with CMW.

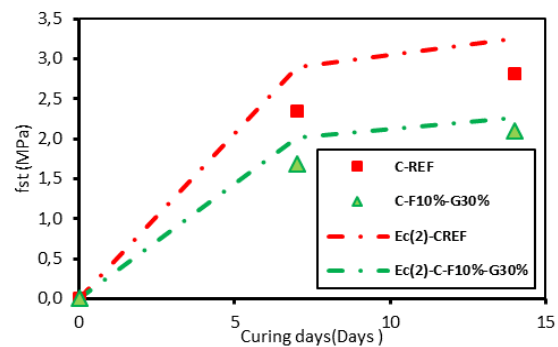


Fig. 7. Variation of Splitting tensile strength of concrete at curing age.

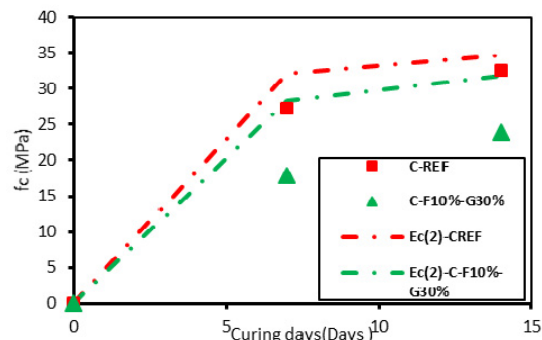


Fig. 8. Variation of Compressive strength with curing age.

Therefore, calibration of the parameter “s” is necessary, based on the experimental results for C-F10%-G30% obtained in this research. The optimization calculation yielded a value of $s=0.6$, which bring a more appropriate prediction. The evaluation of different strengths with calibrated parameter “s” shows a spot-on prediction for the mechanical behaviors of CMWs concrete, Fig. 9 and Fig. 10.

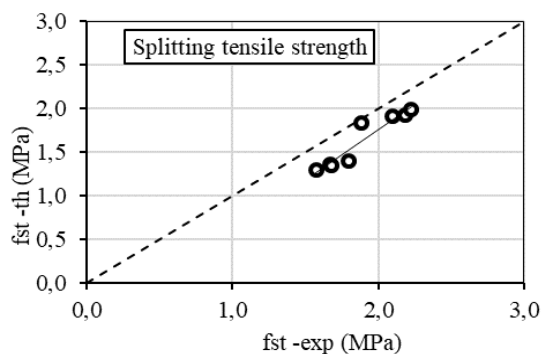


Fig. 9. Experimental Results of the Splitting tensile strength Versus Calculated Values with $s=0.6$.

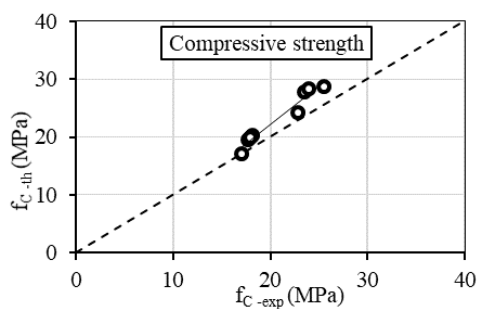


Fig. 10. Experimental Results of the Variation of Compressive strength Versus Calculated Values with $s=0.6$.

III. CONCLUSIONS

In this study, coal mine wastes (CMWs) were used as aggregates in structural concrete in order to examine the mechanical properties. The key findings are as follows:

- The concrete bulk density decreases with increasing coal mine waste particles. This attributed to the lower density of CMW compared to natural aggregate. As the proportion of CMW increases, the concrete porosity increases.

- CMWs affect the workability of concrete. The slump of C-F10%-G30% decreases by 18%, CMW absorb more water mainly due to the presence of mores fines particle size during mixing. As these particles are incorporated into cement pastes, their porosity and the irregularities on CMW surfaces create more surface area for interaction with the cement matrix.

- C-F10%-G30% concrete loses more than 19% of splitting tensile strength and 32% of compressive strength. The disparity in compressive strength between C-F10%-G30% concrete specimens C-REF concrete specimens diminished as the curing period progressed, particularly becoming less distinct at 28 days.

- The calibrated coefficient in EC2 model was introduced to enhance the accuracy of predicting the

compressive and splitting tensile strengths of C-F10%-G30% concrete. It was determined that a coefficient value of 0.6 significantly improved the alignment with experimental result.

As a result, CMW aggerates could be reused to replace natural aggerates in concrete as a partial substitute. However, ensuring that the physical and mechanical properties of concrete require an appropriate amount of replacement. Through this study, we have investigated that the incorporation of 10% CMW sand and 30% CMW gravel in the C40/50 concrete does not significantly affect its mechanical properties.

CONFLICT OF INTREST

The authors declare no conflict of interest.

AUTHOR CONTRIBUTIONS

The authors' contributions to the paper are as follows: Oumayma ABOUTAYBI wrote the paper; BOUYANG YANG revised the paper; all authors approved the final version.

ACKNOWLEDGEMENT

The authors express their gratitude to the Research Fund for Coal and Steel for its financial and logistical support in backing the MINRESCUE Project, RFCS-01-2019 program, with the Proposal number 899518.

REFERENCES

- [1] J. Y. Yoon, J. Y. Lee, and J. H. Kim, “Use of raw-state bottom ash for aggregates in construction materials,” *J Mater Cycles Waste Manag*, vol. 21, no. 4, pp. 838–849, Jul. 2019, doi: 10.1007/s10163-019-00841-5.
- [2] P. Smarzewski and D. Barnat-Hunek, “Mechanical and durability related properties of high-performance concrete made with coal cinder and waste foundry sand,” *Construction and Building Materials*, vol. 121, pp. 9–17, Sep. 2016, doi: 10.1016/j.conbuildmat.2016.05.148.
- [3] M. Singh and R. Siddique, “Effect of coal bottom ash as partial replacement of sand on properties of concrete,” *Resources, Conservation and Recycling*, vol. 72, pp. 20–32, Mar. 2013, doi: 10.1016/j.resconrec.2012.12.006.
- [4] C. R. Santos, R. M. C. Tubino, and I. a. H. Schneider, “Mineral processing and characterization of coal waste to be used as fine aggregates for concrete paving blocks,” *Rev. IBRACON Estrut. Mater.*, vol. 8, pp. 14–24, Feb. 2015, doi: 10.1590/S1983-41952015000100004.
- [5] J. Qiu, Y. Zhou, N. I. Vatin, X. Guan, S. Sultanov, and K. Khemarak, “Damage constitutive model of coal gangue concrete under freeze-thaw cycles,” *Construction and Building Materials*, vol. 264, p. 120720, Dec. 2020, doi: 10.1016/j.conbuildmat.2020.120720.
- [6] V. M. Nguyen, T. B. Phung, D. T. Pham, and L. S. Ho, “Mechanical properties and durability of concrete containing coal mine waste rock, F-class fly ash, and nano-silica for sustainable development,” *Journal of Engineering Research*, p. 100097, May 2023, doi: 10.1016/j.jer.2023.100097.
- [7] M. K. Murukutti and H. Jena, “Synthesis of nano-crystalline zeolite-A and zeolite-X from Indian coal fly ash, its characterization and performance evaluation for the removal of Cs+ and Sr2+ from simulated nuclear waste,” *Journal of Hazardous Materials*, vol. 423, p. 127085, Feb. 2022, doi: 10.1016/j.jhazmat.2021.127085.
- [8] M. Mohebbi, F. Rajabipour, and B. E. Scheetz, “Evaluation of two-atmosphere thermogravimetric analysis for determining the

- unburned carbon content in fly ash,” *Adv. Civ. Eng. Mats.*, p. 20160052, Aug. 2017, doi: 10.1520/ACEM20160052.
- [9] C. Yi *et al.*, “Study on chloride binding capability of coal gangue based cementitious materials,” *Construction and Building Materials*, vol. 167, pp. 649–656, Apr. 2018, doi: 10.1016/j.conbuildmat.2018.02.071.
- [10] C. Wu *et al.*, “A sustainable low-carbon pervious concrete using modified coal gangue aggregates based on ITZ enhancement,” *Journal of Cleaner Production*, vol. 377, p. 134310, Dec. 2022, doi: 10.1016/j.jclepro.2022.134310.
- [11] A. Karimipour, “Effect of untreated coal waste as fine and coarse aggregates replacement on the properties of steel and polypropylene fibres reinforced concrete,” *Mechanics of Materials*, vol. 150, p. 103592, Nov. 2020, doi: 10.1016/j.mechmat.2020.103592.
- [12] D. Li, X. Song, C. Gong, and Z. Pan, “Research on cementitious behavior and mechanism of pozzolanic cement with coal gangue,” *Cement and Concrete Research*, p. 8, 2006.
- [13] B. J. Dalgleish, P. L. Pratt, and E. Toulson, “Fractographic studies of microstructural development in hydrated Portland cement,” *J Mater Sci*, vol. 17, no. 8, pp. 2199–2207, Aug. 1982, doi: 10.1007/BF00543728.
- [14] G. W. Groves, “Portland cement clinker viewed by transmission electron microscopy,” *J Mater Sci*, vol. 16, no. 4, pp. 1063–1070, Apr. 1981, doi: 10.1007/BF00542753.
- [15] A. Kijo-Kleczkowska, M. Szumera, A. Gnatowski, and D. Sadkowski, “Comparative thermal analysis of coal fuels, biomass, fly ash and polyamide,” *Energy*, vol. 258, p. 124840, Nov. 2022, doi: 10.1016/j.energy.2022.124840.
- [16] EUROCODE. [Online]. Available: eurocode-2-design-concrete-structures

Copyright © 2024 by the authors. This is an open access article distributed under the Creative Commons Attribution License ([CC BY-NC-ND 4.0](https://creativecommons.org/licenses/by-nc-nd/4.0/)), which permits use, distribution and reproduction in any medium, provided that the article is properly cited, the use is non-commercial and no modifications or adaptations are made.